Int J Adv Manuf Technol (2013) 66:1231–1245
DOI 10.1007/s00170-012-4402-y

ORIGINAL ARTICLE

Spatter reduction in nanosecond fibre laser drilling using an innovative nozzle

C. A. Biffi · B. Previtali

Received: 28 December 2011 / Accepted: 17 July 2012 / Published online: 31 July 2012

Abstract Pulsed wave fibre lasers are becoming a popular industrial tool in microprocessing due to their many positive features, such as high beam quality, high reliability and high productivity, which are fundamental to machining small, precise features of industrial applications. However, the lasers' use in the machining of ultraprecise features, such as small holes, is hindered by the fact that commercial pulsed wave fibre lasers commonly operate with pulse durations in the nanosecond regime. Such long pulse durations mean that the material is thermally removed, which results in the production of a melted layer and thermal damage in the bulk material. Consequently, the typical thermal defects of the melting regime, such as spattering of recast material around the hole, taper, heat-affected zone and poor hole circularity, are found in materials machined with these lasers. This paper proposes a design for an innovative nozzle that combines the high productivity of nanosecond fibre lasers with an improvement in the quality of the machined holes by reducing the spatter production in titanium laser percussion drilling. The innovative nozzle is based on the suction effect created by the Venturi principle that prevents the deposition of melted and vaporised material on the workpiece surface. The influence of the nozzle configuration and shielding gas on hole quality is investigated after the laser percussion drilling of 0.5-mm-thick titanium sheets, in which the process conditions that allow maximum productivity are used. The innovative nozzle produces a remarkable decrease in spatter on the entrance hole surface without affecting the other quality features, such as hole diameter, circularity and taper, while preserving the high productivity obtainable with a standard nozzle.

Keywords Laser percussion drilling · Fibre laser · Titanium · Nanosecond regime · Spatter reduction · Innovative drilling nozzle

C. A. Biffi (✉)
CNR IENI-Institute for Energetics and Interphases,
Unit of Lecco, Corso Promessi Sposi 29,
23900 Lecco, Italy
e-mail: carlo.biffi@ieni.cnr.it

B. Previtali
Mechanical Engineering Department, Politecnico di Milano,
20156 Milano, Italy
e-mail: barbara.previtali@polimi.it

1 Introduction

Research on precise material processing using long (in nanosecond or ns), short (in picoseconds or ps) and ultrashort (in femtosecond or fs) pulsed wave (PW) lasers has become popular in recent years due to a growing interest in the machining of small features and components in the micromechanics, energy, electronic, aerospace and biomedical sectors. Among the microfeatures that can be obtained by laser microprocessing, the production of high-precision holes is one of the most relevant needs in industrial applications [1–3]. The aerospace industry, in particular, has been successfully employing this technique to drill large numbers of closely spaced cooling holes in turbine engine components, such as airfoils, nozzle guide vanes and combustion chambers [4, 5]. A typical modern engine has approximately 100,000 small-diameter holes (<1 mm) to provide cooling in the turbine blade [6]. Meanwhile, high productivity is needed to create patterns of microvia holes and channels in silicon wafers for microelectronic applications [7]. Producing small holes that are free of spatter and melted material, using highly productive and reliable lasers, would benefit all of these industrial applications. However, it is a challenging task.

A recent advancement in this problem is the application of laser sources characterised by short (ps regime) or ultrashort (fs regime) pulse durations. The main advantage of short and ultrashort laser sources is the minimisation of thermal damage inside the workpiece. As a result, defects caused by excessive heating, such as spattering of remelted material, a large heat-affected zone, cracks and changes in chemical composition, can be minimised with the consequent increase in quality and precision of the machined holes [8]. However, minor productivity (i.e. a low material removal rate) and low industrial implementation (due mainly to high costs and complex equipment) are the two main drawbacks of these laser sources when compared with nanosecond lasers.

Conversely, nanosecond laser sources can be a good compromise between high productivity and acceptable quality in the laser percussion drilling (LPD) process. Due to their rather long pulse width, nanosecond laser sources mainly operate in the melting regime. The presence of melted material reduces the precision of the laser machining and produces defects typical of a melting regime: taper, heat-affected zone, drops of remelted material and spatter on the hole entrance [9]. On the other hand, the high pulse energy and frequency that characterise these laser sources result in a high material removal rate and, consequently, high productivity.

The high productivity of ns laser sources is partially responsible for the recent diffusion of PW nanosecond fibre laser sources, which are on track for becoming a reference industrial tool in laser drilling and microdrilling. These lasers are very simple, easily implemented and reliable and are also characterised by high beam quality, which is an important characteristic when small and precise features are required [10].

However, the large quantity of melted material produced during laser drilling in the ns regime, material that resolidifies as a melted corona around the hole entrance, is one of the unsolved drawbacks of laser drilling with PW ns fibre lasers.

A small number of methods have been proposed in literature to solve the excessive spatter production of these long pulse durations. The most well-known approaches are based on the optimisation of the process parameters to achieve spatter minimisation, but even these methods do not completely remove the spatter and they often do not operate at maximum productivity. The deposition of protective and sacrificial polymeric films, presented in [11], avoids the spatter deposition but contributes to an increase in process time and makes the drilling operations more difficult.

This study proposes two innovative nozzle concepts aimed at reducing the spatter production in LPD using a PW fibre laser operating in the ns regime. The material investigated is commercially pure titanium, which is known for its high tendency to produce spatter and melted material during LPD and for its tendency to be oxidised and contaminated by the ambient atmosphere. Because the productivity of the drilling operation is fundamental to industry, the innovative nozzle is designed to operate at the same drilling time as the standard nozzle and with the same operative conditions in terms of process parameters and shielding gas.

The performance of two nozzle prototypes, when different shielding gases are used, is evaluated and compared, in terms of spatter quantity and hole quality attributes, to the performance of a traditional nozzle commonly used for laser micromachining. The comparison leads to the conclusion that the proposed nozzle can greatly reduce the production of spatter without decreasing productivity when a PW ns fibre laser is used in titanium LPD. Moreover, other quality attributes, such as hole diameter, taper and circularity, are not affected by the use of the innovative nozzle.

2 Design of the innovative nozzle and goals of the study

This study proposes a new nozzle design that reduces spatter on the top surface of drilled holes produced using LPD with a PW nanosecond fibre laser source. During LPD, there is no relative motion between the workpiece and the laser head, and through holes are obtained by regulating the process parameters and drilling time. The material removal mechanism is composed of two parts: removal by vaporisation and by melt ejection. In the nanosecond regime, the contribution of the evaporation phase is significantly less than that of melt ejection [12]. However, the vapour phase is fundamentally important in removing the predominant melt material. The pressure gradients caused by the sudden expansion of the evaporating front (recoil pressure) radially push out the melted material, which is squirted along the hole wall (formally called a recast layer) and at the entrance of the hole (formally called spatter). In the final stage of the percussion drilling process, melted material might also be deposited at the exit of the hole (formally called dross) [13]. In LPD, the drilling head is usually equipped with a conical/convergent nozzle used to force the shielding gas through the nozzle tip. This type of conical nozzle exit performs two tasks: it shields the work area from ambient gas and blows residual melted and vaporised material away from the head optics (see a schematic view in Fig. 1). Figure 1 shows the main structure of the traditional configuration including (1) the protective window on the top surface, (2) the inlet channel for shielding gas adduction and the traditional nozzle (3).

The direct pressure exerted by the shielding gas also contributes to spatter deposition around the entrance hole by splashing molten material radially out of the cavity hole until the through hole is obtained. The relative contribution

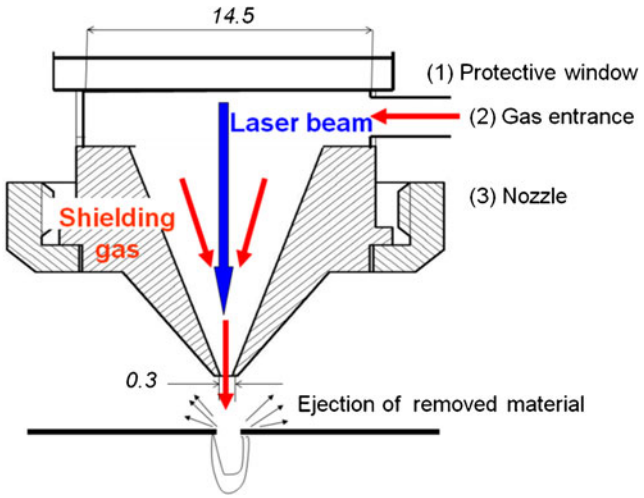

Fig. 1 Schematic of a traditional nozzle used in LPD

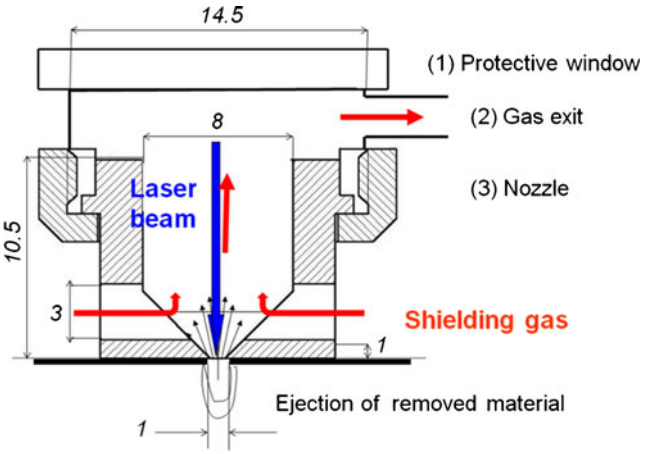

Fig. 3 Schematic of the vertical nozzle

of the two mechanisms, recoil pressure and direct shielding gas pressure, varies with the nature of the shielding gas, the laser parameters, the material composition and thickness of the workpiece and the nozzle geometry and dimensions. But a recast corona of spatter material deposited around the entrance of the hole can always be observed from the beginning of the hole formation.

The goals of the study do not include the accurate modelling of the drilling phase (numerous references can be found in literature [14]). However, it can be useful to observe the way spatter is deposited around a hole entrance in order to study the innovative nozzle design. The sequence of images in Fig. 2 shows the evolution of spatter deposited around a hole during LPD in the ns regime. The sequence was obtained by operating a ns fibre laser and a traditional nozzle (the type shown in Fig. 1) on commercially pure titanium with helium as the shielding gas. Most of the melted material produced in the blind cavity is squirted around the hole wall in a resolidified corona from the beginning of the drilling process, while a portion of material is spread out in the form of microdrops by the sudden expansion of the vapour phase. The corresponding exit hole is spatter-free, as usually occurs in ns LPD [12–16].

Observation of the sequence in Fig. 2 makes two functions of the innovative nozzle clear: it must operate from the beginning of the hole formation and it must remove melted material deposited on the entrance surface. In both of the innovative nozzle prototypes proposed in this study, the removal action is based on the Venturi principle, which means a suction effect is produced by forcing the shielding gas through a constriction. The nozzle design is composed of a closed chamber with inlet and outlet channels. The chamber is bounded on top by protective glass, while the bottom boundary has an orifice for passage of the laser beam. The shielding gas is pumped at a high pressure through the inlet channels, entering the mixing chamber and flowing out through the outlet channels. Due to a restriction in the cross section of the outlet channels, the shielding gas must increase its velocity, reducing its pressure and producing a partial vacuum that sucks out the melted and vaporised material produced on the entrance surface of the hole. The same shielding gas pumped at a high pressure into the nozzle chamber insulates the heated top surface from ambient gases. The final bottom part of the conical chamber must be packed against the top surface of the sheet to ensure sealing of the chamber.

The gas used to generate the suction effect acts also as shielding gas for the work area, which is surrounded by the chamber atmosphere. A similar effect has been discussed in a study by Lei et al. [17] in laser cutting. In that study, a combination of suction and rotational gas flow was used to

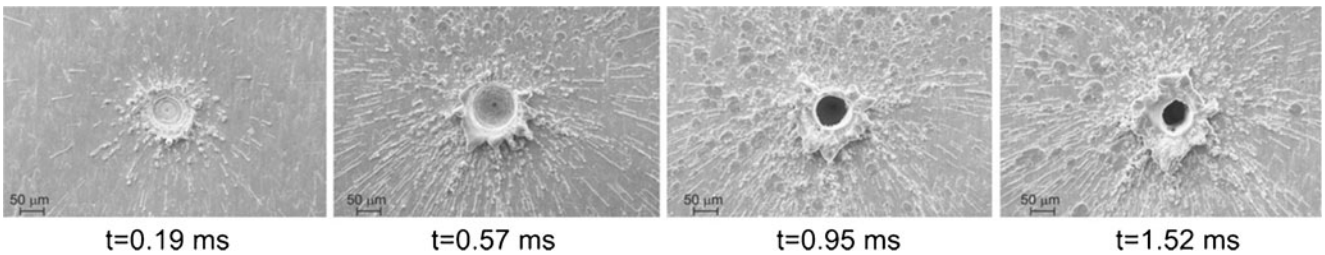

Fig. 2 Spatter evolution on the hole entrance during LPD using a PW ns fibre laser (pulse frequency 80 kHz, pulse energy 0.75 mJ, pulse duration 160 ns)

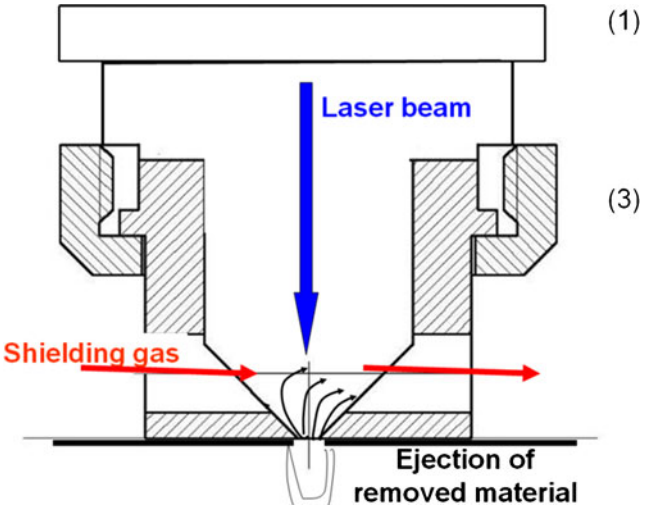

Fig. 4 Schematic of the horizontal nozzle

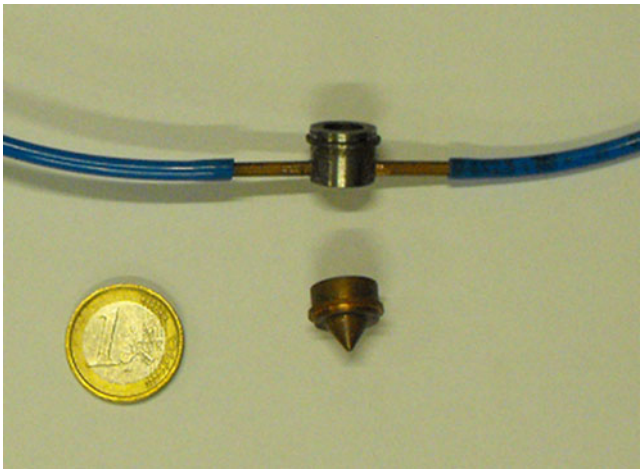

Fig. 5 Chamber used to test the innovative nozzles and the traditional nozzle

achieve the reduction of melted material produced on the exit surface of the laser-cut edge of silicon wafers.

Because the shielding gas loses its ability to force melted material through the hole channel in this new concept, the dross on the bottom surface could eventually increase as a result. In this work, two different inlet–outlet channels layouts are experimentally tested to evaluate their performance in terms of spatter reduction.

The first layout consists of two radial inlet channels that initially force the shielding gas to the centre of the chamber, then out of the chamber through the outlet aperture located just behind the protective mirror, as shown in Fig. 3a. In this configuration, the shielding gas is enriched by the vaporised and melted material moving in a direction opposite the laser beam direction. The shielding gas' path opposite the laser beam is intentionally very short to avoid a potential interaction between the laser beam and the molten material transported by the gas flux (see dimensions in Fig. 3b). Because the drag action of the shielding gas is exerted in the vertical direction, this innovative design is named the vertical nozzle. The two inlet channels in the vertical nozzle are at 180° to guarantee symmetric gas adduction.

Because the vertical direction of the shielding gas enriched by melted material can make the protective window dirty and can strongly interfere with the laser beam in this configuration, the second way to generate a suction effect in the chamber makes use of two horizontal channels, as shown in Fig. 4. The shielding gas is forced into the chamber from the channel on the left (see the arrow direction in Fig. 4a) and goes out through the channel on the right. As before, the protective window and the contact between the nozzle chamber and the top surface of the sheet insulate the work area from ambient gases and shield it with the same gas used to suck away the melted material. Because the suction is primarily horizontal in this second nozzle prototype, the design is named the horizontal nozzle. Figure 4b shows its fundamental dimensions. A filter is placed at the ends of both the horizontal and vertical nozzles to sweep up the removed material.

The goal of this study is to verify the concepts of the two innovative nozzle prototypes, horizontal and vertical, and compare their performance with the performance of a standard

Table 1 Main characteristics of the pulsed fibre laser used in the experiments

Constant parameters	Emission wavelength (nm)	1,064
	Beam quality factor	1.7
	Collimated laser beam diameter (mm)	5.9
Controllable parameters	Pump current (%)	0–100
	Pulse frequency range (kHz)	20–80
Derived parameters	Nominal maximum average power (W)	50
	Nominal maximum pulse energy (mJ)	1.2
	Nominal maximum peak power (kW)	8.5
	Pulse duration range (FWHM) (ns)	100–160

Table 2 Fixed factors in the experimental investigating drilling time

Average power (W)	50
Pump current (%)	100
Gas pressure (bar)	7
Focus position	Top surface
Focal length (mm)	60
Spot diameter (μm)	23
Working distance (with the traditional nozzle) (mm)	0.5

Table 3 Variable factors in the experiment investigating drilling time

Nozzle type	Traditional, horizontal, vertical
Shielding gas	Helium, argon
Pulse frequency (kHz)	20-35-50-65-80

nozzle used in the microdrilling process, here called the traditional nozzle. The basis of comparison is primarily the quantity of spatter left on the top surface during laser drilling with a laser source characterised by high productivity (i.e. a short drilling time). Therefore, the comparison is carried out using the laser process condition that is able to guarantee the shortest drilling time. The comparison of the nozzle performances is performed using statistical tools such as the analysis of variance (ANOVA) and Tukey's multiple comparison tests [18]. The definitive mechanical design of the nozzle configurations, shapes and dimensions, using fluid dynamic computation, was deliberately postponed until after this exploratory feasibility analysis was concluded.

3 Experimental design

LPD was performed in this experiment using a PW IPG Photonics fibre laser. This laser source is an industrial tool used for micromachining. Its most noticeable features are good beam quality, high pulse energy, high efficiency, compact dimensions and easy maintenance. However, due to its long pulse duration and high available energy, it is known to work mainly within the melting regime and produces a high quantity of spatter and recast material [15, 16].

The main characteristics of this laser source are listed in Table 1. The laser's controllable parameters are the pump current and pulse frequency, while the pulse duration varies within the range of 100–160 ns. The pump current and pulse frequency determine the average power, peak power and pulse energy, as reported in [15].

A Laser Mech drilling head equipped with a 60-mm focal lens and a standard coaxial nozzle for the adduction of shielding gas was used. In this configuration, the nominal diameter corresponding to the focus position is approximately

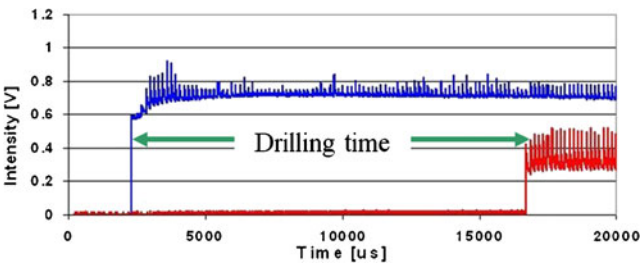

Fig. 6 Representative example of the procedure used to measure drilling time

Table 4 Process conditions at the minimum drilling time used in the experiment evaluating the innovative nozzle's performance

Fixed factors	Average power (W)	50
	Pump current (%)	100
	Focal position	Top surface
	Working distance (with the traditional nozzle) (mm)	0.5
	Gas pressure (bar)	7
	Pulse frequency (kHz)	80
	Drilling time T_{drill} (ms)	1.5
Variable factors	Nozzle type	Traditional, horizontal, vertical
	Shielding gas	Helium, argon

23 μm. An Aerotech linear motion stage was used to create the pattern of through holes.

The material investigated was commercially pure (CP) grade 2 titanium, cold rolled in 0.5-mm-thick sheets. CP titanium was chosen because it is widely used in the biomedical and aerospace sectors, where LPD is a standard procedure used to obtain a dense pattern of holes.

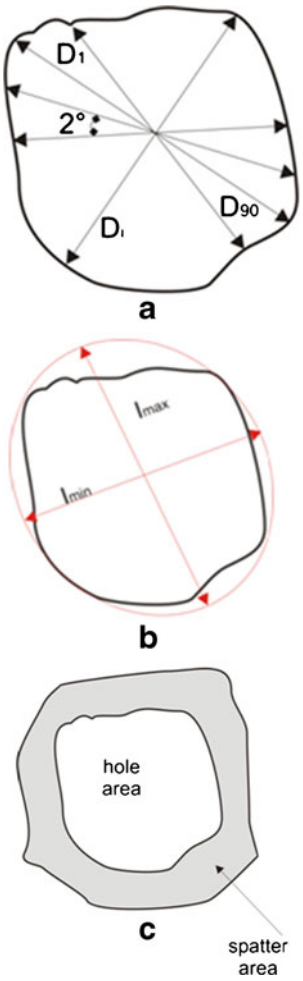

Fig. 7 Definitions of the quality attributes of an LPD hole: **a** mean diameter, **b** aspect, **c** spatter area

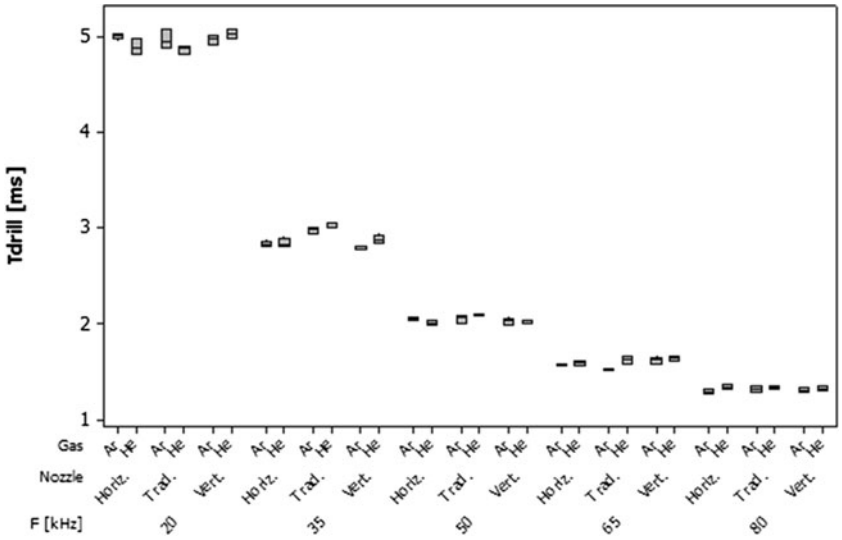

Fig. 8 Box plot of the drilling time in the investigated process conditions

The investigated nozzle types were the traditional nozzle, depicted in Fig. 1, and the two previously introduced innovative nozzle prototypes. The horizontal and vertical nozzles were machined with EDM from a stainless steel round bar, and the lateral tubes were made of copper (see the physical prototypes in Fig. 5).

In addition to investigating nozzle designs, the experiment also explored the effect of the other process parameters that are supposed to influence the LPD of CP titanium. These parameters include the shielding gas due to its fundamental role in removing spatter and protecting the work area from contact with ambient gases. Two inert gases, argon and helium, were selected because they are commonly used in the laser processing of titanium due to their low reactive behaviour [19]. The laser process parameters were also taken into consideration. The purpose of this work is to show that highly productive PW fibre lasers are valid tools for use in the laser drilling of CP titanium as long as excessive spatter production is reduced. Consequently, the process parameters that allow the creation of holes at maximum productivity were sought for all three nozzles. Their productivity was evaluated by measuring the drilling time.

The experiment was carried out in two steps: (1) an evaluation of the drilling time as a function of different process conditions (i.e. shielding gas type and pulse frequency, which were known to affect process productivity [15]) was performed for all three nozzle types and (2) the performance of the two proposed prototypes in terms of maximum productivity was compared to the traditional nozzle based on hole quality.

A complete factorial design was performed to study the effect of the main process parameters, including shielding gas, pulse frequency, F, and nozzle type on drilling time, T_{drill}, in accordance with the fixed and variable factors shown in Tables 2 and 3, respectively.

The drilling time, T_{drill}, is defined as the requested time used to produce through holes. In this work, T_{drill} was measured using two fast infrared photodiodes positioned on the top and bottom surfaces of the titanium sheets to be drilled.

Table 5 Regression table for the drilling time model

Regression analysis						
$\ln T_{\text{drill}}$ (ms)=4.47−0.96 ln F (kHz)						
Predictor	Coeff	SE coeff	T		P	
Constant	4.4745	0.01566	285.69		0.000	
ln F (kHz)	−0.95971	0.004087	−234.80		0.000	
Analysis of variance						
Source	–	- DF	SS	MS	F	P
Regression		1	32.555	32.555	55,150	0.000
Residual	Error	144	0.085	0.001		
	Lack of fit	3	0.003	0.001		
	Pure error	141	0.082	0.001	1.76	0.157
Total		145	32.640			

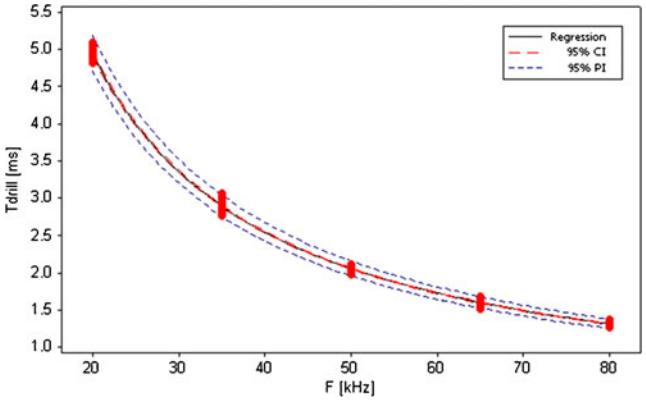

Fig. 9 Confidence (CI) and prediction interval (PI) at 95 % probability in the regressive model for drilling time

The first photodiode acquires the reflected laser beam from the top surface of the titanium sheet when the drilling process starts. The second fast photodiode then acquires the signal produced by the direct laser beam when it emerges from the exit hole, immediately after the through hole is obtained. The drilling time was evaluated as the difference between the two signals, as shown in Fig. 6 [15].

Each measurement was performed five times to estimate the experimental error. A regressive model for the drilling time was proposed to define the level of pulse frequency that minimises T_{drill} and maximises productivity.

Once the conditions at minimum drilling time were found for the three nozzles, a second factory plan was designed and executed to investigate the effects of two factors, nozzle type and shielding gas, and compare the performances of the proposed prototypes. Table 4 anticipates the results of the first experiment, showing the conditions at maximum productivity used in the second experiment corresponding to 80 kHz. Each process condition was tested five times. The ANOVA technique and Tukey's test were used to identify significant differences among the three nozzles. According to the Bonferroni criterion, a 5 % family alpha error was considered in the analysis of both experiments [18].

Due to the small dimensions of the machined holes (a few tenths of a micron [15]), the hole images were captured using scanning electron microscopy (SEM). SEM was also used due to the necessity of having a high depth of field in the scan of the hole morphology to identify spatter on the entrance surface. In particular, a secondary electron signal (SE) was adopted during the image acquisition because this signal is generally used to identify precisely the morphology of a sample surface. The use of an optical microscope was attempted for this purpose, but its depth of field was not sufficient for obtaining clear hole images.

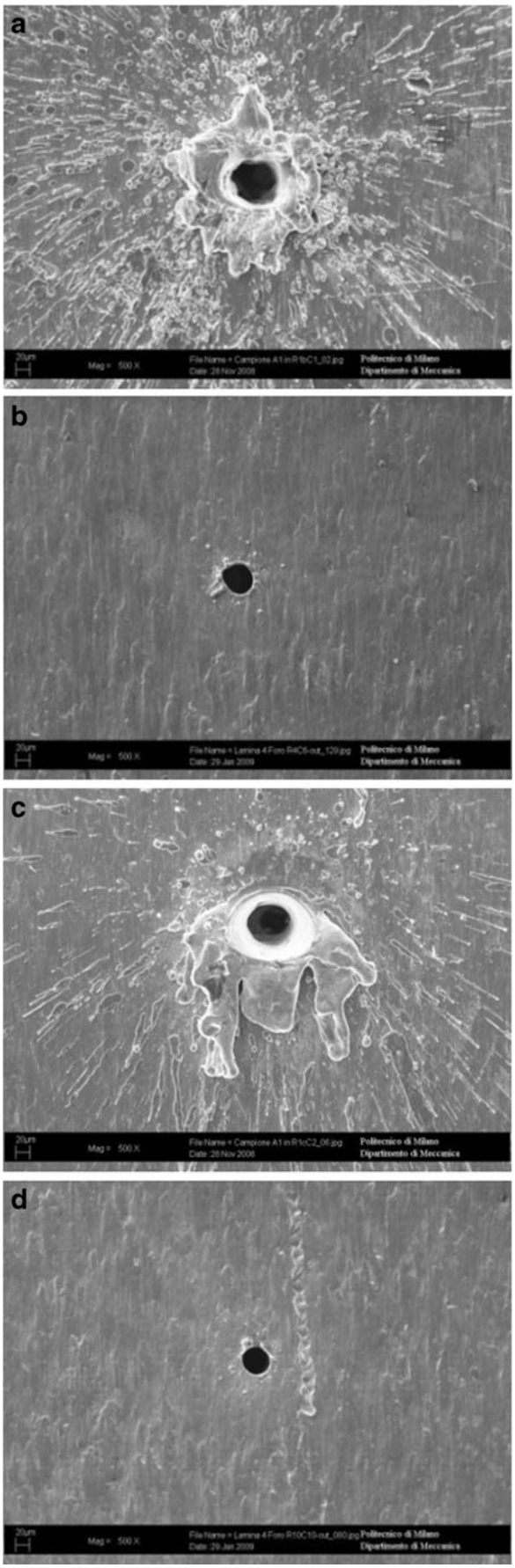

Fig. 10 Representative images of the holes machined with the traditional nozzle: entrance and exit surfaces, respectively, in using helium (**a**–**b**) and argon (**c**–**d**) ▶

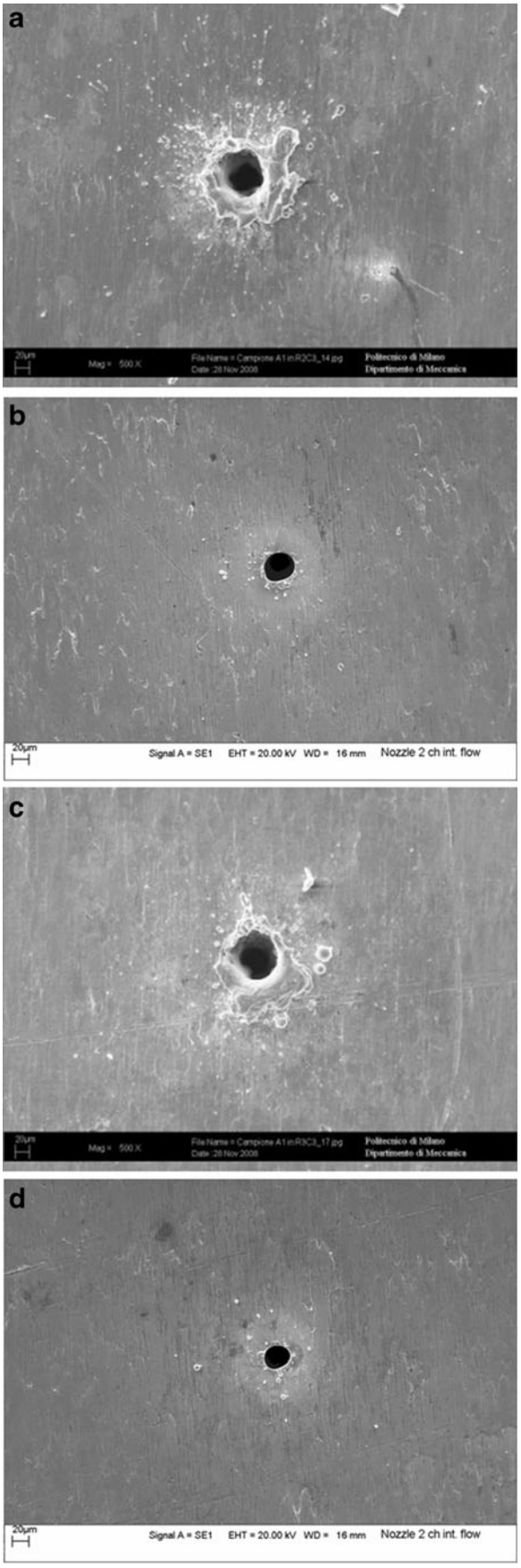

Fig. 11 Representative images of the holes machined with the vertical nozzle: entrance and exit surfaces, respectively, using helium (**a**–**b**) and argon (**c**–**d**)

The following quality features were evaluated to characterise the laser-drilled holes (Fig. 7):

1. Mean diameter (D_{top} and D_{bottom}): the average length of 90 diameters measured at 2° intervals and passing through the hole centroid, evaluated on the top and bottom surfaces (see Fig. 7a). It can be calculated as follows:

$$D = 1/90 \sum_{n=1}^{90} D_i \tag{1}$$

   This type of measurement can be adopted when the hole profile is not completely regular.
2. Aspect (A_{top} and A_{bottom}): an indicator of hole circularity obtained using the ratio between the minor and major axes of the equivalent ellipse of the hole evaluated on the top and bottom surfaces (see Fig. 7b). It can be calculated as follows:

$$A = I_{max}/I_{min} \tag{2}$$

   The aspect is 1 when the hole is perfectly circular; otherwise, the aspect is greater than 1.
3. Spatter ratio ($R_{spatter}$): the ratio between the area of spatter and the area of the corresponding hole on the top surface. The area of spatter is the measurement of the extension of the spatter around the hole periphery reduced by the area of the hole (see Fig. 7c) [15, 16]. Only spatter on the top surface is considered because it is nearly absent on the bottom surface. Although some drops are present on the top surface of the titanium sheets, their contribution is not considered in the measurement of the area of spatter.
4. Taper (T): the average inclination of the inner wall of the hole, calculated as follows:

$$T(\text{in radian}) = \text{arctg}\left[\left(D_{top} - D_{bottom}\right)/2\,t\right] \tag{3}$$

   where D_{top} and D_{bottom} are the top and bottom hole diameter, respectively, and t is the thickness of the drilled sheet.

The measurements of the hole quality features defined above were conducted on the images, acquired for the top and bottom holes, making use of commercial software for the image analysis. The procedure for the measurement of D_{top}, D_{bottom}, A_{top} and A_{bottom} was fully automated, and the software was able to identify the external profiles of the top and bottom holes to produce the defined quantities. The

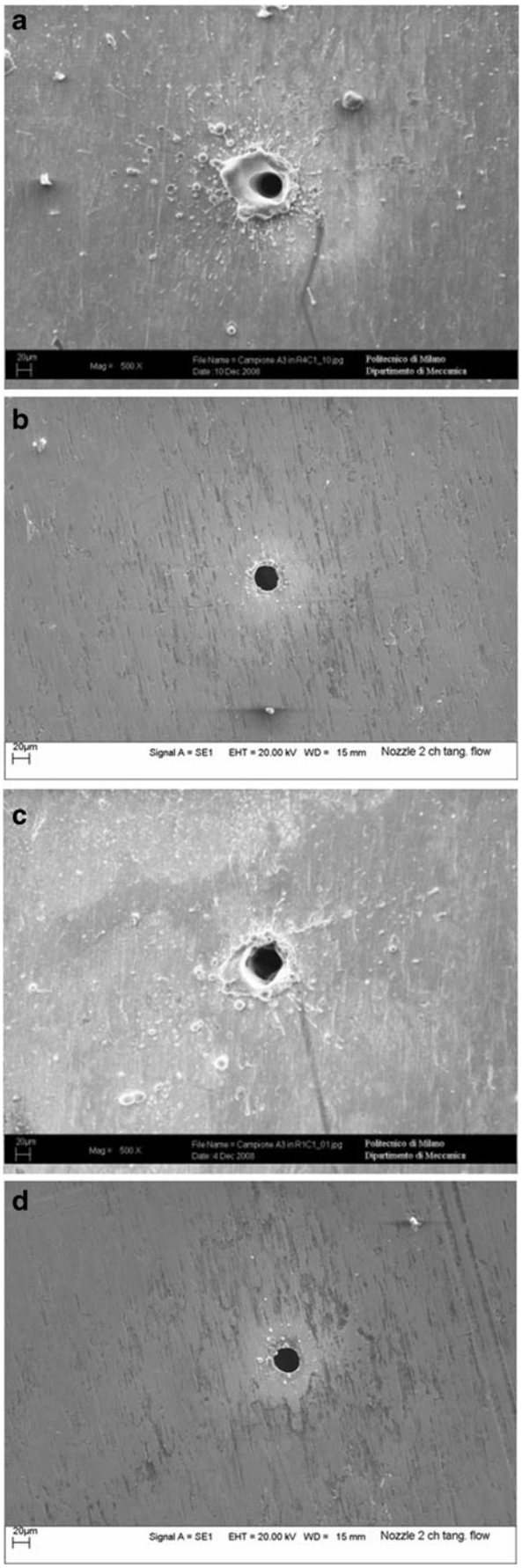

Fig. 12 Representative images of the holes machined with the horizontal nozzle: entrance and exit surfaces, respectively, using helium (**a**–**b**) and argon (**c**–**d**)

recognition and measurement of the area of the top holes was also fully automatic, but the profile of the spatter deposited on the top surface was manually selected because automatic recognition was impossible. Once the profile was identified, the software returned the extension of spatter. The spatter area was then obtained by subtracting the top hole area from the measured spatter extension; $R_{spatter}$ could then be evaluated.

4 Analysis and discussion of results

4.1 Drilling time analysis and identification of the process condition at maximum productivity

Figure 8 shows the box plot of the measured drilling time under the investigated process conditions indicated in Table 3. The figure shows that T_{drill} decreases from approximately 5 to 1.5 ms as the pulse frequency F increases from 20 to 80 kHz. The influence of the shielding gas and the nozzle type is not significant, as the ANOVA analysis confirms. In particular, the two innovative nozzles do not significantly change T_{drill}, which is almost the same for the three investigated nozzles. This is an encouraging result because it shows that the high productivity of LPD is not changed by the use of the innovative nozzles.

A regressive model with T_{drill} as a function only of the pulse frequency, F, is proposed in Eq. 4, and the corresponding regression table is reported in Table 5.

$$T_{drill}(\text{in millisecond}) = 87.36/F^{0.96}(\text{in kilohertz}) \quad (4)$$

The relationship between T_{drill} and F that best fits the experimental data and satisfies the regression hypotheses is a double logarithmic function, as shown in Fig. 9.

In terms of the fibre laser used here, as reported in [15], the average power increases when the frequency increases up to 50 kHz, then remains almost constant for higher values of pulse frequency. Correspondingly, the pulse energy is almost 1.2 mJ up to 50 kHz and then decreases to 0.8 mJ at 80 kHz.

The steep decrease in drilling time when the frequency increases in the first part of the curve in Fig. 9 is due to the increase in the average power. Consequently, an increase of the heat input into the workpiece is obtained that promotes faster melting and evaporation. When the pulse frequency is further increased, the average power remains constant, while the pulse energy decreases, causing a progressive loss of efficiency in the drilling process that is most likely emphasised by the excessive production of plasma [20]. Therefore,

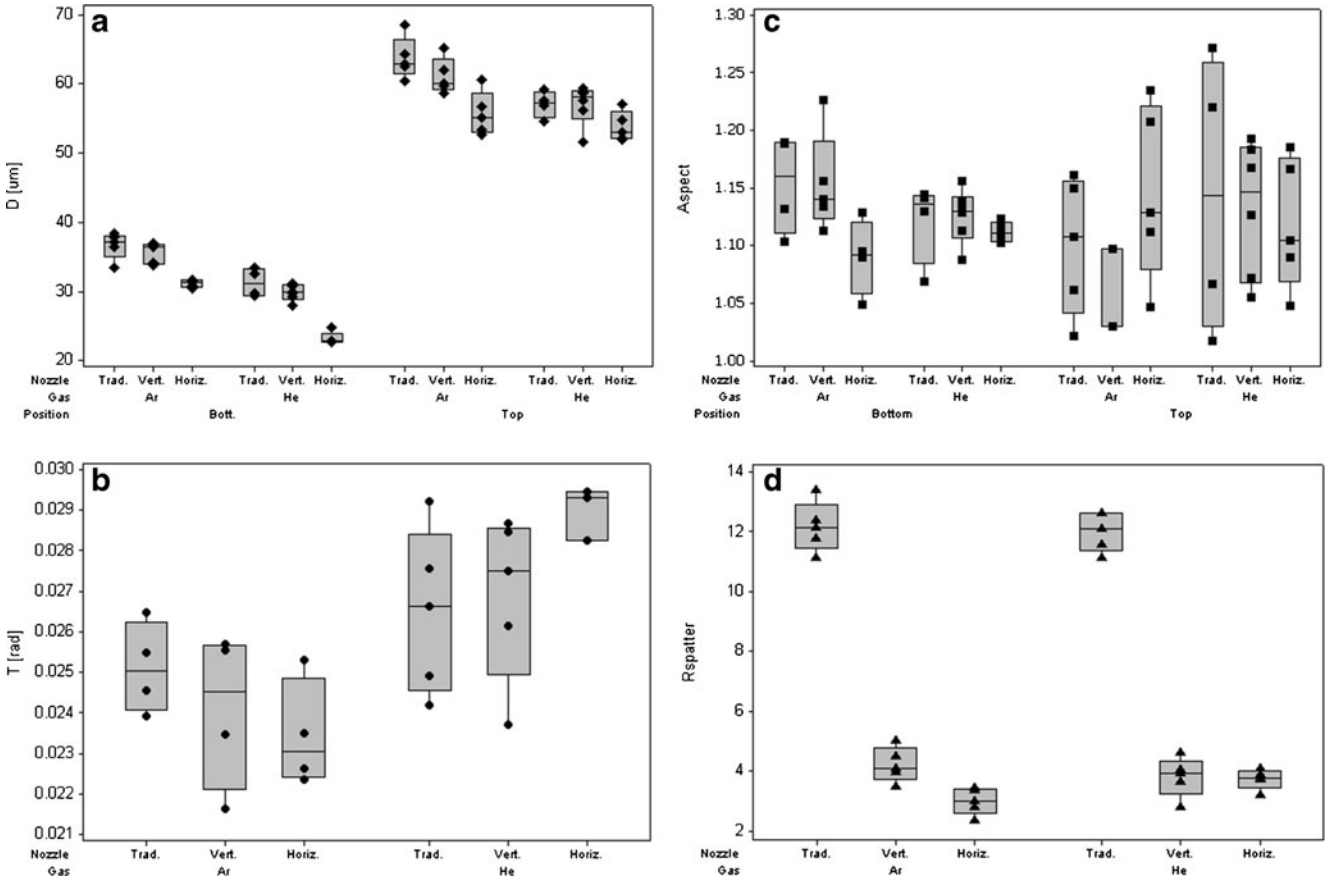

Fig. 13 Box plot of the quality attributes for the investigated conditions: **a** top and bottom diameter, **b** taper, **c** top and bottom aspect, **d** spatter ratio

the reduction in drilling time is less important at higher frequencies than at lower frequencies so that the shortest drilling time is obtained at an 80-kHz pulse frequency (95 % confidence interval is ±0.01 ms). The high repeatability of the microdrilling process can also be taken into account, being on the order of half a millisecond.

The process parameters described in Table 4, together with a pulse frequency of 80 kHz, were used in the next experiment, and the goal of which is to compare the innovative nozzles with the traditional nozzle under the maximum productivity condition.

4.2 Comparison of nozzles performances

Figure 10 shows the entrance and exit holes obtained using the traditional nozzle, with helium and argon as shielding gases, under the process condition, allowing the maximum productivity. The entrance holes show a large amount of spatter and a relevant quantity of melted drops deposited around the periphery of the drilled holes. The extent of the spatter is relevant because the presence of such a large amount of melted material around the hole periphery on the top surface, as well as the large numbers of melted drops spread out in the surrounding region, certainly decreases the quality of the laser-drilled holes. In addition, the great quantity of spatter confirms that long pulse durations produce important thermal effects, not only in the form of spatter but also in possible recast material and a heat-affected zone inside the hole [16]. Upon visual inspection, helium seems to produce more drops of melted material than argon, though the difficulty in measuring the spread of the drops makes evaluation difficult. However, exit holes are free of spatter and drops of melted material, as expected [15, 16].

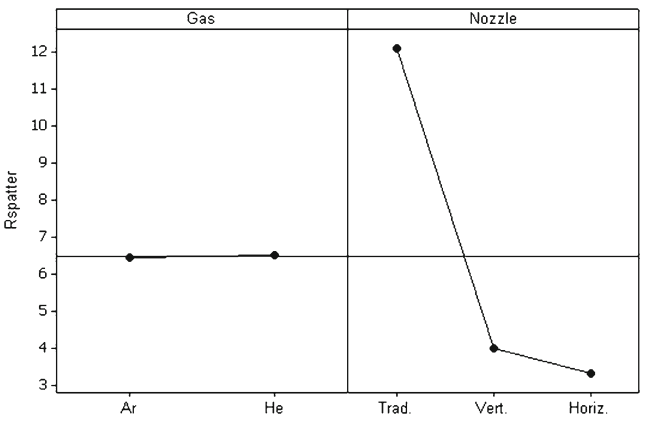

Fig. 14 Main effect plot for spatter ratio

Table 6 Analysis of variance and Tukey's simultaneous tests for spatter ratio

Analysis of variance for $R_{spatter}$						
Source	DF	Seq	SS adj	MS	*F*	*P*
Gas	1	0.028	0.028	0.028	0.08	0.786
Nozzle	2	475.345	475.345	237.672	643.93	0.000
Gas × nozzle	2	1.818	1.818	0.909	2.46	0.106
Error	24	8.858	8.858	0.369		
Total	29	486.049	486.049			
S=0.607533	*R*-sq=98.18 %	*R*-sq(adj)=97.80 %				
Tukey's simultaneous tests, response variable $R_{spatter}$						
All pairwise comparisons among levels of gas						
Gas = Ar subtracted from:						
Gas	Difference of means	SE of difference	*T* value		Adj *P* value	
He	0.06083	0.2218	0.2742		0.7863	
All pairwise comparisons among levels of nozzle						
Nozzle = trad. subtracted from:						
Nozzle	Difference of means	SE of difference	*T* value		Adj *P* value	
Vert.	−8.095	0.2717	−29.79		0.0000	
Horiz.	−8.754	0.2717	−32.22		0.0000	
Nozzle = vert. subtracted from:						
Horiz.	−4.832	0.6835	−7.0700		0.0000	

Figures 11 and 12 show the entrance and exit holes obtained with the innovative nozzles at the same drilling time, respectively. The spatter around the holes on the top surface is still present, but it is significantly less than the spatter on the corresponding hole created with the traditional nozzle. In addition, a few drops of melted material can be observed around the entrance of the holes thanks to the suction effect generated by the shielding gas flux.

Moreover, the exit holes are free of spatter. The new concept for the two nozzle prototypes does not modify the behaviour of the drilling laser beam on the exit side, which remains spatter-free.

The box plots in Fig. 13 allow a preliminary analysis of the experimental data to be performed. At first glance, there is a large difference between the top and bottom diameters, with the top diameters being larger (see Fig. 13a). Therefore, the drilled holes should have a conic shape (see Fig. 13b). Moreover, both the bottom and top holes are not perfectly circular because their aspect is far from 1. Figure 13c shows that in all the experimental conditions, the aspect data are not only greater than 1 but also highly dispersed. This is particularly true in the case of the aspect data measured on the top surface, most likely due to the presence of spatter, which makes the circularity measurement more uncertain. Spatter is present on the laser-drilled holes with the traditional nozzle, while a significant reduction is observed after the use of both the innovative nozzles.

A more accurate analysis is needed, based on tools such as the ANOVA and Tukey's multiple comparison tests that can give statistical significance to the differences observed in Fig. 13. In particular, the effectiveness of the nozzle design on the reduction of spatter must be verified.

Concerning the $R_{spatter}$ value, the ANOVA gives evidence that when the significance of the gas and nozzle types is tested, the nozzle is the only significant factor affecting the value, while shielding gas and the interaction between the two are not (see *p* values in Table 7). The traditional nozzle produces a spatter area 12.1 times larger than the hole area (the 95 % confidence interval is 11.59–12.61). The adoption of the vertical and horizontal nozzles reduces this ratio to 4.0 and 3.3, respectively (3.56–4.45 and 2.96–3.70 are their 95 % confidence intervals). However, the analysis of the main plots in Fig. 14 does not give evidence of a significant

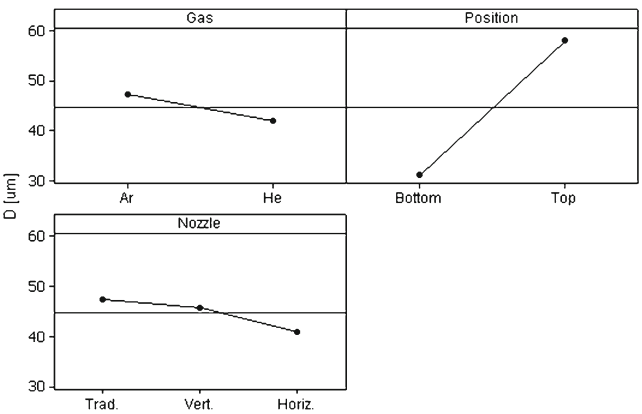

Fig. 15 Main effect plot for hole diameter

difference between the vertical and horizontal nozzles because their average values are very close. It should be noted that the real difference in terms of spatter reduction between the traditional nozzle and the vertical and horizontal nozzles is higher than the data reported in Fig. 13d. In fact, the large quantity of drops present on the laser-drilled holes created by the traditional nozzle is not included into the spatter ratio. On the contrary, the presence of drops is significantly reduced when the two proposed innovative nozzles are used.

Conversely, the Tukey's test comparison in Table 6 shows that the vertical and horizontal nozzles are slightly different in terms of $R_{spatter}$, while both strongly differ from the traditional nozzle. The mechanism of spatter removal is more effective in the horizontal design because the spatter area is only 3.3 times the laser-drilled hole area. Compared to the vertical flux, the horizontal gas flux seems to work better because it results in higher spatter reduction and does not involve the protective glass placed directly in contact with the sucked melted material, as the vertical nozzle does. Both nozzles should also guarantee the prevention of excessive oxidation with the ambient atmosphere in the drilled area because they fill the chamber full of inert gas.

To study the ability to produce holes as large as the holes laser-drilled by the traditional nozzle, three factors are compared in the ANOVA: the hole position (on the top and bottom surfaces), the shielding gas used and the nozzle type. The position was considered as a variable input factor because the preliminary data investigation (see Fig. 13) has shown a probable tapering effect. All three factors are statistically significant, but their interactions are not, as reported in the main effect plots of Fig. 15 and the ANOVA in Table 7.

The position was found to be the most affecting one among the inputs, confirming the conical shape of the drilled holes. As is often reported in the case of long pulse laser drilling, the top diameters are significantly larger than the bottom diameters when the focus position is on the top surface, due to the overheating exerted by the melted material deposited around the entrance hole during the drilling process [15, 16, 21].

Table 7 Analysis of variance and Tukey's simultaneous tests for hole diameter

Analysis of variance for D (μm)						
Source	DF	Seq	SS adj	MS	F	P
Gas	1	430.8	430.8	430.8	92.21	0.000
Nozzle	2	427.2	427.2	213.6	45.72	0.000
Position	1	10,856.1	10,856.1	10,856.1	2323.84	0.000
Gas × nozzle	2	3.3	3.3	1.6	0.35	0.704
Gas × position	1	19.0	19.0	19.0	4.07	0.049
Nozzle × position	2	5.0	5.0	2.5	0.53	0.590
Gas × nozzle × position	2	29.5	29.5	14.8	3.16	0.051
Error	48	224.2	224.2	4.7		
Total	59	11,995.1	11,995.1			
S=2.16140	R-sq=98.13 %	R-sq(adj)=97.70 %				
Tukey's simultaneous tests, response variable D (μm)						
All pairwise comparisons among levels of gas						
Gas = Ar subtracted from:						
Gas	Difference of means	SE of difference	T value		Adj P value	
He	−5.359	0.5581	−9.603		0.0000	
All pairwise comparisons among levels of nozzle						
Nozzle = trad. subtracted from:						
Nozzle	Difference of means	SE of difference	T value		Adj P value	
Vert.	−1.395	0.6835	−2.042		0.1133	
Horiz.	−6.228	0.6835	−9.112		0.0000	
Nozzle = vert. subtracted from:						
Horiz.	−4.832	0.6835	−7.070		0.0000	
All pairwise comparisons among levels of position						
Position = bottom subtracted from:						
Position	Difference of means	SE of difference	T value		Adj P value	
Top	26.90	0.5581	48.21		0.0000	

Table 8 Analysis of variance and Tukey's simultaneous tests for taper

Analysis of variance for *T* (rad)						
Source	DF	Seq	SS adj	MS	*F*	*P*
Gas	1	0.0000569	0.0000643	0.0000643	22.56	0.000
Nozzle	2	0.0000012	0.0000021	0.0000010	0.36	0.702
Gas × nozzle	2	0.0000171	0.0000171	0.0000085	2.99	0.074
Error	19	0.0000542	0.0000542	0.0000029		
Total	24	0.0001294				
S=0.00168849	*R*-sq=58.13 %		*R*-sq(adj)=47.11 %			
Tukey's simultaneous tests, response variable *T* (rad)						
All pairwise comparisons among levels of gas						
Gas = Ar subtracted from:						
Gas	Difference of means	SE of difference	*T* value		Adj *P* value	
He	0.003256	0.000685	4.750		0.0001	
All pairwise comparisons among levels of nozzle						
Nozzle = trad. subtracted from:						
Nozzle	Difference of means	SE of difference	*T* value		Adj *P* value	
Vert.	−0.000313	0.000801	−0.3902		0.9199	
Horiz.	0.000417	0.000858	0.4856		0.8789	
Nozzle = Vert. subtracted from:						
Horiz.	0.000729	0.000858	0.8498		0.6775	

The difference between holes obtained using argon and helium is also statistically significant. Drilling in argon produces a larger hole than in helium. The ANOVA allows the significance of the nozzle design on the hole diameters to also be investigated. A significant difference in the diameters obtained using the different nozzle types is confirmed.

However, only the Tukey's simultaneous test in Table 8 allows verification that the traditional and vertical nozzles produce holes that are not significantly different, while the holes produced by the horizontal nozzle are significantly smaller. This result is true for both the top and bottom diameters, although the interaction factors are not shown in the Tukey's analysis for the sake of brevity. This result means that if the same diameters must be obtained, the traditional nozzle can be substituted with the vertical nozzle because holes with comparable diameters can be obtained while significantly reducing R_{spatter}.

The conical shape of the laser-drilled hole can be further investigated if the effect of the process parameters and nozzle type on the hole inclination is tested. The inclination of the hole wall, based on the top and bottom diameter measurements, seems to be affected neither by the nozzle nor by the interaction between the nozzle and the shielding gas, but it is affected by the shielding gas (see ANOVA in Table 8 and the main effect plot in Fig. 16). In particular, the innovative nozzle design has no influence on the tapering effect.

Moreover, holes obtained using helium are more inclined than those obtained using argon. Therefore, if holes with the same diameters to those obtained with the traditional nozzle have to be obtained, the vertical nozzle design should be chosen because it guarantees about 30 % of the spatter at the same diameter. However, the choice of shielding gas affects the diameter value and hole inclination because holes obtained using argon are larger and less inclined.

As preannounced by the data snooping, the circularity is not affected by the choice of nozzle and process parameters. Indeed, the large data variance does not allow the effect of input parameters to be shown. As is often reported in such studies, the ANOVA in Table 9 concludes that the hole circularity does not seem to vary when the nozzle, gas and position are considered. The holes have an average aspect of 1.12 (the 95 % confidence interval is 1.10–1.14), which is

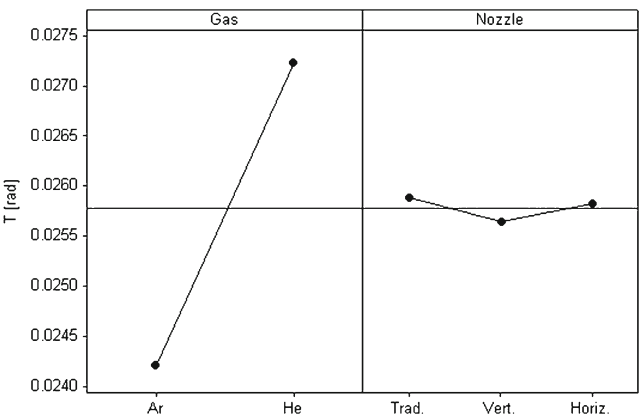

Fig. 16 Main effect plot for taper

Table 9 Analysis of variance and Tukey's simultaneous tests for hole aspects

Analysis of variance for A

Source	DF	Seq	SS adj	MS	*F*	*P*
Gas	1	0.000337	0.001200	0.001200	0.39	0.536
Nozzle	2	0.002535	0.004684	0.002342	0.76	0.474
Position	1	0.000727	0.001628	0.001628	0.53	0.471
Gas × nozzle	2	0.001158	0.001113	0.000557	0.18	0.835
Gas × position	1	0.005639	0.006711	0.006711	2.18	0.147
Nozzle × position	2	0.012445	0.014789	0.007394	2.40	0.102
Gas × nozzle × position	2	0.015203	0.015203	0.007602	2.47	0.096
Error	44	0.135523	0.135523	0.003080		
Total	55	0.173567				
S=0.0554983	*R*-sq=21.92 %		*R*-sq(adj)=2.40 %			
Tukey's simultaneous tests, response variable *A*						
All pairwise comparisons among levels of gas						
Gas = Ar subtracted from:						
Gas	Difference of means	SE of difference	*T* value		Adj *P* value	
He	0.009370	0.01501	0.6243		0.5357	
All pairwise comparisons among levels of nozzle						
Nozzle = trad. subtracted from:						
Nozzle	Difference of means	SE of difference	*T* value		Adj *P* value	
Vert.	−0.02144	0.01853	−1.157		0.4848	
Horiz.	−0.01695	0.01809	−0.937		0.6201	
Nozzle = vert. subtracted from:						
Horiz.	0.004489	0.01853	0.2423		0.9682	
All pairwise comparisons among levels of position						
Position = bottom subtracted from:						
Position	Difference of means	SE of difference	*T* value		Adj *P* value	
Top	−0.01091	0.01501	−0.7270		0.4711	

not perfectly circular. Specifically, the innovative nozzles do not decrease the circularity of the entrance and exit holes.

5 Conclusions

This paper proposes a solution to reduce the amount of spatter produced when a fibre laser operating in the ns regime is used in the LPD of a titanium sheet. As a result, a good compromise between the high productivity of such a laser source and the large thermal effects resulting from the long pulse regime can be found in situations where a dense pattern of holes must be obtained. The solution is based on a new nozzle design that, thanks to the Venturi effect, provides suction of the melted and vaporised material produced during the LPD process on the top surface. Two configurations of the innovative nozzle were investigated, horizontal and vertical. Both configurations maintain the role of protecting and shielding the work area from atmospheric gases, a fundamental task when titanium is processed.

Two experiments were designed and executed to compare the new nozzles to a traditional nozzle under maximum productivity conditions. The analysis of the experimental data by means of statistical tools has led to the following main conclusions:

- Neither of the innovative nozzles modifies the drilling time; instead, drilling time is affected mainly by the pulse frequency. Therefore, the maximum productivity condition that leads to the minimum drilling time can be independently set by the nozzle type and the shielding gases.
- Both of the innovative nozzles cause the spatter around the entrance hole to be greatly reduced. The traditional nozzle produces a spatter area 12 times larger than the entrance hole area. In contrast, the area of the spatter is three and four times the entrance hole area in the case of the horizontal and vertical nozzles, respectively. Drops around the spatter are also significantly less frequent in both of the innovative configurations compared to the

traditional nozzle. As observed in the traditional nozzle, neither spatter nor drops are present on the bottom surface around the exit hole.

- The horizontal nozzle is preferred over the vertical nozzle because it ensures the highest spatter reduction and does not force a dirty gas towards the protective window. However, the hole diameters are slightly smaller than those obtained with the traditional and vertical nozzles.
- The other defects, taper and poor circularity, that are common in nanosecond regime LPD when maximum productivity is sought are unaffected by the nozzle design. In particular, the taper depends only on the shielding gas used. However, the high dispersion of aspect data does not allow the dependence of circularity on process parameters to be observed.
- The proposed nozzle prototypes can be considered of great interest and relevance to industrial applications when a dense pattern of microholes, blind or through, must be produced on flat surfaces at high productivity. Spinnerets and filters are two representative examples of this type of industrial application.
- A possible limitation of the proposed innovative nozzle prototypes is the need to keep the nozzle in contact with the top surface of the sheet to be drilled, which consequently requires fixed focal distances. Otherwise, further improvements to achieve industrialisation can now be introduced. In particular, movable optics or telescopic nozzles may be adopted to simultaneously ensure contact with the surface and variable optic parameters.

References

1. Chichkov BN, Momma C, Nolte S, Von Alvensleben F, Tünnermann A (1996) Short-pulse laser ablation of solid targets. Opt Commun 129(1–2):134–142
2. Pronko PP, Dutta SK, Squier J, Rudd JV, Du D, Mourou G (1995) Machining of sub-micron holes using a femtosecond laser at 800 nm. Opt Commun 114(1–2):106–110
3. Tam SC, Willams R, Yang LJ, Jana S, Lim LEN, Lau MWS (1995) A review of the laser processing of aircraft components. J Mater Process Tech 23:177–194
4. Dijk MHHV, Vlieger GD, Brouwer JE(1989) Laser precision hole drilling in aero-engine components. Proceedings of the sixth international conference on lasers in manufacturing, Springer, Berlin 237–247
5. Corfe AG (1983) Laser drilling of aero-engine components. Proceedings of the first international conference on lasers in manufacturing, Springer, Berlin 31–38
6. Naeem M, Chinn J (2008) Advancement in laser drilling for aerospace gas turbines. Proceedings of PICALEO 197–202
7. Hainsey RF, Hooper AE, Swenson EJ, Nashner MS (2006) Recent advances in laser micromachining for semiconductors and microfluidic applications. Proceedings of ICALEO203–212
8. Meijer J, Du K, Gilner A, Hoffmann D, Kovalenko VS, Masuzawa T, Ostendorf A, Poprawe R, Schulz W (2002) Laser machining by short and ultrashort pulses, state of the art and new opportunities in the age of the photons. CIRP Ann Manuf Technol 51(2):531–550
9. Bandyopadhyay S, Sundar JK, Sundararajan G, Joshi SV (2002) Geometrical features and metallurgical characteristics of Nd:Yag laser drilled holes in thick IN718 and Ti-6Al-4V sheets. J Mater Process Tech 127:83–95
10. Hallgren C, Reimers H, Chakarov D, Gold J, Wennerberg A (2003) An in vivo study of bone response to implants topographically modified by laser micromachining. Biomaterials 24:701–710
11. Low DKY, Li L, Byrd PJ (2003) Spatter prevention during the laser drilling of selected aerospace materials. J Mater Process Tech 139:71–76
12. Kudesia SS, Solana P, Rodden W, Hand DP, Jones J (2005) Appropriate regimes of laser drilling models containing melt eject mechanisms. J Laser Appl 14:159–164
13. Yilbas BS (1997) Parametric study to improve laser hole drilling process. J Mater Process Technol 70:264–273
14. Zhang Y, Faghri A (1999) Vaporization, melting and heat conduction in the laser drilling process. Int J Heat Mass Transf 42:1775–1790
15. Biffi CA, Previtali B (2008) Spatter reduction during titanium microdrilling using pulsed fiber laser. Proceedings of ICALEO 27–36
16. Biffi CA, Lecis N, Previtali B, Vedani M, Vimercati G (2010) Fiber laser microdrilling and its effect on material microstructure. Int J Adv Manuf Tech 983–994
17. Lei H, Yi Z, Chenglong M (2009) Technological study of laser cutting silicon steel controlled by rotating gas flow. Optic Laser Tech 41:328–333
18. Montgomery DC (2000) Design and analysis of experiments, 5th edn. Wiley, New York
19. Rodden WSO, Kudesia SS, Hand DP, Jones JDS (2001) Use of "assist" gas in the laser drilling of titanium. J Laser Appl 13 (5):204–208
20. Ancona A, Röser F, Rademaker K, Limpert J, Nolte S, Tünnermann A (2008) High speed laser drilling of metals using a high repetition rate, high average power ultrafast fiber CPA system. Opt Express 16:8958–8968
21. Bandyopadhyay S, Gokhale H, Sarin Sundar JK, Sundararaian G, Joshi SV (2005) A statistical approach to determine process parameter impact in Nd:YAG laser drilling of IN718 and Ti-6Al-4V sheets. Opt Lasers Eng 43:163–182